

# Thermalization Calorimetry: A simple method for investigating glass transition and crystallization of supercooled liquids

Bo Jakobsen,<sup>1, a)</sup> Alejandro Sanz,<sup>1</sup> Kristine Niss,<sup>1</sup> Tina Hecksher,<sup>1</sup> Ib H. Pedersen,<sup>1</sup> Torben Rasmussen,<sup>1</sup> Tage Christensen,<sup>1</sup> Niels Boye Olsen,<sup>1</sup> and Jeppe C. Dyre<sup>1</sup>  
*“Glass and Time”, IMFUFA, Department of Sciences, Roskilde University, Postbox 260, DK-4000 Roskilde, Denmark*

We present a simple method for fast and cheap thermal analysis on supercooled glass-forming liquids. This “Thermalization Calorimetry” technique is based on monitoring the temperature and its rate of change during heating or cooling of a sample for which the thermal power input comes from heat conduction through an insulating material, i.e., is proportional to the temperature difference between sample and surroundings. The monitored signal reflects the sample’s specific heat and is sensitive to exo- and endothermic processes. The technique is useful for studying supercooled liquids and their crystallization, e.g., for locating the glass transition and melting point(s), as well as for investigating the stability against crystallization and estimating the relative change in specific heat between the solid and liquid phases at the glass transition.

Keywords: Thermalization, calorimetry, supercooled liquid, glass transition, crystallization

## I. INTRODUCTION

Einstein is often quoted for stating that if you have just one choice of measurement, go for the specific heat. The point is that this quantity by integration determines the entropy, the free energy, etc, i.e., all of the relevant thermodynamics. Indeed, calorimetry is a standard method throughout the scientific, technical, and industrial world, which has been commercially available in many different versions for more than 50 years<sup>1–6</sup>. Modern calorimetry is highly sophisticated and measures with unprecedented accuracy and, even more importantly, on smaller and smaller samples<sup>7–9</sup>. Thus nanocalorimetry is now becoming routinely available, which is essential for ultrafast measurements and expensive samples, e.g., in modern molecular biology or advanced material science<sup>8–10</sup>. At the same time there is, however, a need for “quick and dirty” calorimeters in some branches of physics and chemistry in which fast answers for initial investigations are more important than accuracy.

Our group<sup>11</sup> has for many years conducted research into viscous liquids and the glass transition. “What is the glass transition temperature?” is the first question one asks when investigating a new liquid. Here accuracy is not important, but speed, flexibility, and simplicity are. This paper presents our simple “Thermalization Calorimetry” (*TC*) method, which has proven to be a useful tool for preliminary investigations of glass-forming liquids.

The *TC* method is based on recording the temperature as a function of time for a system that is slowly cooled or heated with a heat current that depends linearly on the temperature of the sample because it derives from heat conduction to (or from) the surroundings. The *TC* technique is simpler to implement than traditional differential scanning calorimetry (*DSC*) because the linearity between heat current and temperature is obtained by passive insulation of the sample and because no heating device is required.

In *TC* changes in specific heat, exothermic, and endothermic processes, are observed by plotting the rate at which the temperature changes with time,  $\frac{dT(t)}{dt}$ , versus the temperature,

---

<sup>a)</sup>Electronic mail: boj@dirac.ruc.dk

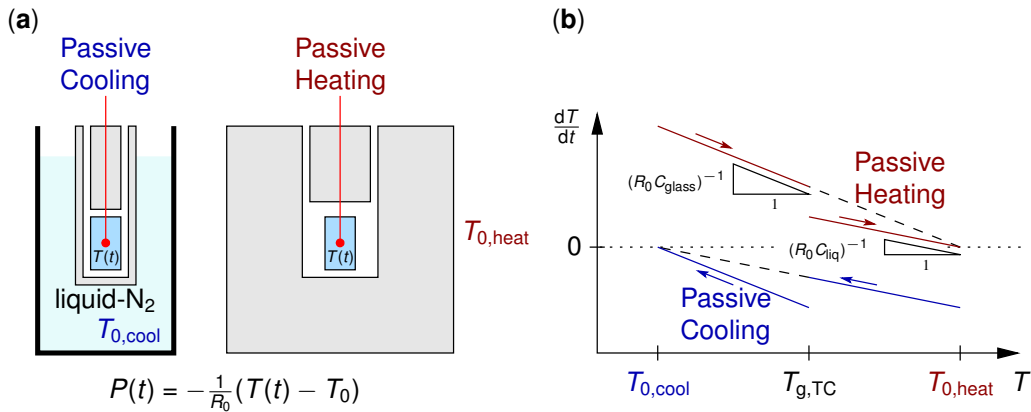


FIG. 1. Illustration of the two typical modes of operation of the TC technique and the expected  $(T, \frac{dT}{dt})$ -traces for a glass forming liquid.

**a)** The experimental setup. The gray region is insulating material, the red line and dot illustrate the thermocouple inserted in the sample (marked by blue). The basic assumption is that the thermal power into the sample,  $P(t)$ , is proportional to the difference between the temperature of the surroundings,  $T_0$ , and the sample temperature,  $T$ , with proportional constant  $1/R_0$  in which  $R_0$  is the thermal resistance of the insulating material. **Left** part illustrates slow passive cooling of a sample placed in an insulating container inserted directly into the cooling agent (which is normally liquid nitrogen).  $T_0$  is here the temperature of the cooling agent, i.e., 77 K. **Right** part illustrates a slow passive heating of a pre-cooled glassy sample using a block of insulation material.  $T_0$  is here the (room) temperature outside the insulating material.

**b)** Expected  $(T, \frac{dT}{dt})$ -traces for the two protocols applied to a glass-forming liquid with constant specific heat in the liquid ( $C_{\text{liq}}$ ) and the glass ( $C_{\text{glass}}$ ). The curves change slope and show a “jump” at the glass transition temperature,  $T_{g,TC}$ , due to the change in specific heat between the equilibrium supercooled liquid and the glass. The dashed lines are guides to the eye, extending to  $(T_0, 0)$  in the both cases. See Sec. II for details on the interpretation.

$T(t)$ . Such a plot reveals a wealth of thermodynamic information about the sample, its glass transition, crystallization, etc. The TC method is inspired by simple experiments conducted more than 40 years ago by our colleague J. Højgaard Jensen<sup>12</sup> for demonstrating the glass transition in propanols. Since then the TC method (nicknamed “*The Red Box*”) has been a workhorse for years in the *Glass and Time* group. TC is our standard tool for initial studies of new glass-forming liquids by which we locate the glass-transition temperature and investigate the liquid’s stability against crystallization. Furthermore, TC has turned out to be excellent for teaching purposes. It has been used for numerous student projects at all levels from high school to master’s project, in which the method’s simplicity and ease of adaptation has allowed for studies of samples ranging from amorphous drugs to candy and amber.

The paper is structured as follows: Section II introduces the technique and how to interpret TC data. Examples of applications to glass transition and crystallization are given in Sec. III. Finally, Sec. IV presents a short discussion of pros and cons of the technique and perspectives on adaptation to further applications. The appendices give details on the experimental protocols (Appendix A), on the technical implementation of the technique (Appendix B), as well as a discussion of a simple Tool-type<sup>13</sup> model of the glass transition that is useful also for teaching purposes, (Appendix C).

## II. THE THERMALIZATION CALORIMETRY (TC) TECHNIQUE

Figure 1 illustrates the two ways we normally use the TC technique. As mentioned in the Introduction, the TC method is based on heating or cooling via a passive, insulating material; this results in a heat current that is proportional to the temperature difference between

sample and surroundings. During this process the temperature and its time derivative are recorded. In the following we briefly describe the TC technique and the two protocols normally used for studying glass-forming molecular liquids. The technique can be adapted to other conditions and protocols, some of which are briefly discussed in Sec. IV.

A convenient and commonly used TC protocol for characterizing glass-forming molecular liquids is a “fast quench” to the glassy state followed by the “slow heating” of thermalization. Alternatively, the liquids may also be studied under “slow cooling” and subsequent “slow heating” (examples of all combinations are given in Sec. III A). Figure 1 illustrates the “slow heating” and “slow cooling” arrangements. For details on the experimental protocols associated with these experiments, see Appendix A.

In all experiments the liquid is positioned in a small glass test tube (8 mm in diameter and 40 mm in length) and a thermocouple-based thermometer is submerged in the sample. Liquid nitrogen provides an excellent cooling agent for studying most molecular glass-forming liquids, and room-temperature is likewise a convenient target temperature for heating experiments. A fast quench is performed by dipping the test tube into a jar of boiling liquid nitrogen. For the slow heating protocol, from liquid nitrogen temperature to room temperature, the pre-cooled sample is subsequently quickly transferred to a block of expanded polystyrene (EPS) — pre-cooled to establish the temperature gradient — with  $\approx 5$  cm wall thickness. This combination of sample size and insulation block gives typical initial heating rates of a few tenths of a Kelvin per second ( $\approx 10$  K/min). For “slow cooling” similar cooling rates can be obtained by insulating the test tube from the liquid nitrogen by a few millimeters of insulating material. The temperature range and cooling/heating rates can easily be modified by using other cooling/heating agents and insulating arrangements.

Two different implementation of the TC technique exist in our lab: the original version based on analog electronics for differentiation and averaging of the data (used for the majority of data presented in this paper) and a more recent digital version in which the differentiation is performed after digitization of the  $T(t)$  signal. The implementations of both versions are discussed in Appendix B.

### Interpretation of $(T, \frac{dT}{dt})$ -graphs

The data analysis of the TC technique is based on plotting  $(T, \frac{dT}{dt})$ -graphs. The basis of the interpretation is that the rate at which the sample changes its temperature,  $\frac{dT(t)}{dt}$ , is inversely proportional to the specific heat of the sample,  $C$ , at a given heat current input,  $P(t) = \frac{dQ}{dt}$ . The onset is the definition of the specific heat:

$$\Delta T = \frac{1}{C}Q \quad (1)$$

where  $\Delta T$  is the temperature increase after introducing some amount of heat,  $Q$ . Taking the time derivative leads to the desired relation:

$$\frac{dT(t)}{dt} = \frac{1}{C} \frac{dQ}{dt} = \frac{1}{C} P(t). \quad (2)$$

In the long time limit this holds for the macroscopic sample investigated here (neglecting heat diffusion in the sample).

A fundamental assumption of the analysis is that the heat current into the sample is proportional to the difference between the target temperature,  $T_0$ , and the sample temperature:

$$P(t) = -\frac{1}{R_0}(T(t) - T_0) \quad (3)$$

where  $R_0$  is the thermal resistance in the experiment (assumed to be temperature independent).

Combining the above equations (Eq. 2 and 3) leads to the following differential equation:

$$\frac{dT(t)}{dt} = -\frac{1}{R_0C}(T(t) - T_0). \quad (4)$$

This is easily solved analytically for constant  $R_0C$ ,<sup>14</sup> but that is *not* the route we take for analyzing data. Instead, direct information is obtained by plotting  $\frac{dT}{dt}$  as a function of  $T$  (see Fig. 1). For constant  $C$  the graph is a straight line with slope  $-\frac{1}{R_0C}$  ending at the point  $(T, \frac{dT}{dt}) = (T_0, 0)$ . The instantaneous value of  $-\frac{1}{R_0C}$  at a given  $(T, \frac{dT}{dt})$  point can be found as the slope of the secant from that point to  $(T_0, 0)$ .

The ability to directly monitor changes in specific heat as a function of temperature is particularly useful for investigating glass-forming liquids, because a signature of the glass transition is a change in specific heat, as illustrated on Fig. 1. This change of specific heat is the result of the “freezing in” of the structural degrees of freedom when the liquid falls out of equilibrium to form a glass<sup>15</sup>. The glass transition has the appearance of a second-order phase transition in the Ehrenfest sense, but as is well known the transition is a dynamic phenomenon and the transition temperature changes (logarithmically) with cooling rate<sup>16</sup>.

Exothermic and endothermic processes likewise give a very clear TC signal because they dramatically change the overall  $(T, \frac{dT}{dt})$ -trace by, respectively, a large increase in  $\frac{dT}{dt}$  and  $\frac{dT}{dt}$  approaching 0.

### III. APPLICATIONS

The TC technique is useful for studying different aspects of supercooled liquids. In the following we present examples of how the technique can be used for locating the glass-transition temperature and for studying crystallization.

#### A. Data from two glass-forming liquids

Two typical molecular glass-forming liquids, tetramethyl-tetraphenyl-trisiloxane (commercial name: DC704) and glycerol, have been investigated<sup>17</sup>. The former has been studied in great detail by the *Glass and Time* group by several techniques<sup>18–22</sup>; the latter is a prototypical glass-forming liquid.

##### 1. Measurements

Figure 2 shows  $(T, \frac{dT}{dt})$ -traces from measurements on the two liquids. The figure includes data for “slow heating after quench cooling” and temperature cycles consisting of a “slow cooling” followed by a “slow heating”. The heating curves start in thermal equilibrium at liquid nitrogen temperature (77.3 K). Initially they show a sharp increase in  $\frac{dT}{dt}$  deriving from the transfer of the sample to the insulating block. A small  $\frac{dT}{dt}$  overshoot is often observed, depending on how fast this transfer is performed and how well the insulating block has been pre-equilibrated (see Appendix A). The trace quickly becomes approximately linear in time. The cooling curves likewise start in equilibrium at room temperature with a fast decrease in  $\frac{dT}{dt}$  until equilibrium cooling conditions have been established.

A clear signature of the glass transition (at 215 K for DC704 and 194–195 K for glycerol) is seen during both heating and cooling as changes in the slope of the  $(T, \frac{dT}{dt})$ -trace (compare Fig. 1). Note that the signature of the glass transition is very robust, also when changing cooling protocol, and that the cooling and heating curves are consistent.

Small sharp peaks close to the glass transition often appear on the cooling curves, as seen at  $\approx 205$  K for DC704. We believe that these stem from crack formation in the sample as it solidifies. The cooling curve for glycerol display a problem sometimes encountered

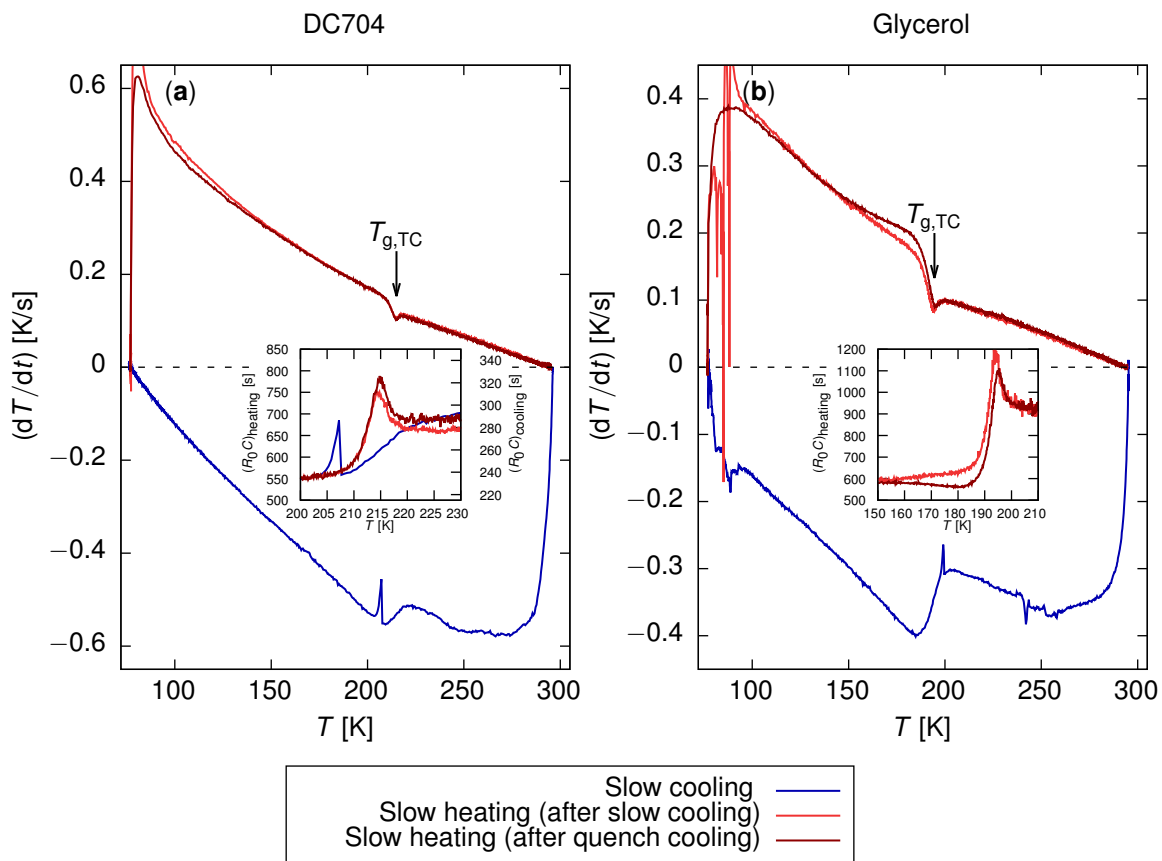


FIG. 2. Glass transition studied by TC. Measurements on two typical glass forming liquid, (a) DC704 and (b) glycerol (see Ref. 17 for details on the samples). The dark red curves show heating after a fast quench to liquid nitrogen temperature. The light red and blue curves show a cycle of slow cooling to liquid nitrogen temperature (blue curves) followed by slow heating to room temperature (light red curves). The glass transition is clearly seen in both cooling and heating. The inserts show the apparent specific heat represented as the  $R_0C$  value from Eq. (4) (notice the different y-axis for the heating and cooling  $R_0C$  curves, due to the difference in  $R_0$  between the two protocols).

in cooling. The  $(T, \frac{dT}{dt})$ -trace on the low temperature side of the glass-transition does not “point to” the  $(T_0, 0)$  point. We attribute this to the rather primitive insulating arrangement used; if cooling curves are needed for accurately evaluating the relative change in specific heat (discussed below), a better arrangement can be constructed; however, the identified glass-transition temperature is not affected by this.

## 2. Analysis

Even though the glass transition is well resolved in the  $(T, \frac{dT}{dt})$ -traces, it covers a non-negligible temperature range. In order to derive an experimentally well-defined number we define the experimental TC glass-transition temperature,  $T_{g,TC}$ , to be the temperature of the local minimum on the heating curve.

The  $T_{g,TC}$  values are given in Table I together with  $T_g$  and characteristic times at  $T = T_{g,TC}$  from studies<sup>21,23</sup> of the equilibrium shear modulus ( $\tau_G$ ), dielectric ( $\tau_\epsilon$ ), and specific heat ( $\tau_{C_I}$ ). It is seen that the  $T_{g,TC}$  is at slightly higher temperature than the traditionally defined  $T_g$  of  $\tau = 100$  s. In fact, the glass-transition temperature is not uniquely

	$T_g$				$\tau$ at $T_{g,TC}$			$\frac{\Delta C}{C_{liq}}$	
	$T_{g,TC}$	$T_{g,C_l}$	$T_{g,\epsilon}$	$T_{g,G}$	$\tau_{C_l}$	$\tau_\epsilon$	$\tau_G$	TC	Lit.
DC704	215 K	211.5 K	210 K	208 K	4.8 s	1.4 s	0.3 s	0.2	0.2 [20]
Glycerol	194–195 K		186 K	180 K		1.9 s	0.03 s	0.3	0.4–0.5 [24]

TABLE I. Glass transition temperature ( $T_g$ ) from TC and three dynamic response functions (shear modulus,  $G(\omega)$ , dielectric constant,  $\epsilon(\omega)$ , and specific heat,  $C_l(\omega)$ ), characteristic timescale ( $\tau$ ) of the same three response functions at  $T_{g,TC}$ , and relative change in specific heat between glass and liquid ( $\Delta C/C_{liq} = (C_{liq} - C_{glass})/C_{liq}$ ). The values are based on the TC data shown in Fig. 2 and from measurements<sup>21,23</sup> of the three dynamic quantities on the thermo-viscoelastic (metastable) equilibrium viscous liquid.  $T_g$  from TC is found as described in the main text, from the local minimum on the heating curve, whereas for the three response functions  $T_g$  is defined as the temperature at which the characteristic time is 100 s.<sup>25</sup>  $\tau$  at  $T_{g,TC}$  is found from the same dynamical data for the three response functions.  $\Delta C/C_{liq}$  from TC is found from the data shown on the insert of Fig. 2 and is compared to values from literature.

defined; different experimental methods has different characteristic time scales at the same temperature — therefore a slightly different  $T_g$ .

The apparent specific heat, represented as  $R_0C$ , can be found from the data using Eq. (4), and is shown in the insets of Fig. 2. The change in specific heat between the liquid and glass is clear in this representation. The above discussed experimentally determined  $T_{g,TC}$  corresponds to the maximum of the observed overshoot in the specific heat. From the  $R_0C$  data an estimate of the relative change in specific heat between glass and liquid can be found; these data are given in Table I together with literature data. It is seen that the TC technique provides a good first estimate of this quantity. For DC704 the cooling and heating curves give consistent results. This could not be checked for glycerol due to the problems with the  $(T, \frac{dT}{dt})$ -trace endpoint for the cooling measurement discussed in Sec. III A 1.

A significant difference between the heating curves of quenched and slowly cooled glycerol is observed. This difference can be rationalized by the difference in thermal history and hence the glasses formed. However, depending on the properties of the liquid studied the signature of thermal history will be more or less visible, as is seen when comparing the DC704 and glycerol data. A simple model that captures the essence of glass formation, including the differences between fast and slow cooling, is presented in Appendix C.

## B. Glass-transition temperature of glycerol-water mixtures

Liquid-liquid mixtures in general and alcohol-water solutions in particular have been widely explored, not only in fundamental studies, but also for their potential applicability<sup>26</sup>. Here we take as a case study a family of glycerol-water mixtures. Glycerol-water is a well-known miscible system in which the crystallization ability of water is highly suppressed. For this reason, many authors have used this mixture to address fundamental questions of the physics of pure liquid water<sup>27,28</sup>. Glycerol-water mixtures have also received much interest due to their utilization as bioprotective agents of cells and proteins<sup>29,30</sup>.

Four glycerol-water mixtures (72, 80, 90, 100% volume fraction of glycerol) were prepared by mixing anhydrous glycerol (purity  $\geq 99.5\%$ ) with distilled and deionized pure water (Arium 611®). Estimates of the glass-transition temperature of pure water give values lower than those corresponding to pure glycerol (the exact glass-transition temperature of water is not known as water crystallizes by spontaneous homogeneous crystallization in the supercooled regime before reaching the glass transition, see, e.g., Ref. 31). One expects that miscible mixtures of glycerol-water are characterized by a monotonic decrease of  $T_g$  when the water content increases. Figure 3(a) shows the  $(T, \frac{dT}{dt})$ -traces from slow heating of initially quenched glycerol-water mixtures. The signature of the glass transition shifts

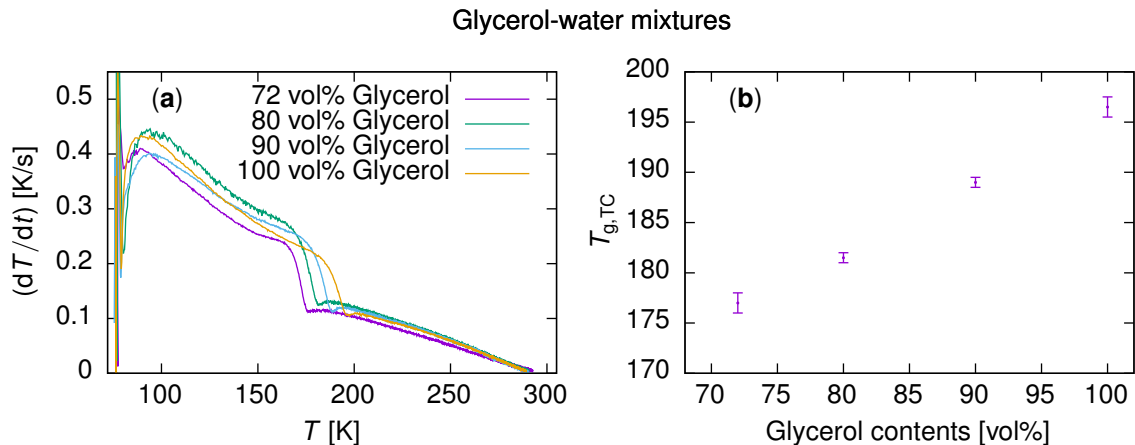


FIG. 3. Glass-transition temperature of glycerol-water mixtures studied by the TC technique. (a)  $(T, \frac{dT}{dt})$ -traces for glycerol-water mixtures with varying glycerol contents. (b) Glass-transition temperature,  $T_{g,TC}$ , as a function of glycerol content given as the volume fraction of glycerol. Error bars are estimated from the shape of the local minimum in the  $(T, \frac{dT}{dt})$ -trace defining  $T_{g,TC}$ .

	$T_m$	$T_{g,TC}$
1-Octyl-1-methylpyrrolidinium TFSI	260 K	194–195 K
Diethylene glycol	260 K (262.7 K [32])	178–181 K
Acetone	176.5–177.5 K (178.8 K [33])	

TABLE II. Melting,  $T_m$ , and glass-transition temperature,  $T_{g,TC}$ , determined from TC on three substances<sup>17</sup> (raw TC data shown on Fig. 4). Numbers in parenthesis are from the literature.

towards lower temperatures with the water content, as expected. Figure 3(b) shows how the values of  $T_{g,TC}$  become lower when the volume fraction of glycerol decreases.

### C. Crystallization and melting

The TC technique is well suited for studying the stability of a supercooled liquid against crystallization and locating the melting point of the crystal.

In pure systems, at sufficiently low temperatures the thermodynamically stable form is crystalline. When liquids are supercooled and situated between the melting temperature ( $T_m$ ) and the glass-transition temperature ( $T_g$ ), these are susceptible to crystallization. This transition of a metastable liquid into a crystal is controlled by several factors like the rate of nucleation and growth of the crystallites, viscosity, and the heating or cooling rate to which the system is subjected. Most liquids are easily supercooled to form a glass when cooled fast enough. Some systems, however, recrystallize during heating at similar rates from the glassy state. The transformation of supercooled liquids into crystals (known as “cold crystallization”) is of great interest in fundamental science as well as in industry<sup>34</sup>.

Data on the following three liquids with different crystallization behavior is presented in the following<sup>17</sup>: 1-octyl-1-methylpyrrolidinium TFSI (OctPyr-TFSI) (a room-temperature ionic liquid), diethylene glycol (a typical molecular glass-forming liquid), and acetone (a small-molecule solvent). Figure 4 shows TC data for the crystallization of these liquids and Table II summarizes the melting and glass transition temperatures derived from TC.

Figure 4(a) shows a heating curve for OctPyr-TFSI initially quenched in liquid nitrogen. Going from low to high temperature the glass transition is seen at 194–195 K, followed by crystallization of the supercooled liquid around 230 K (which is, of course, an exothermic

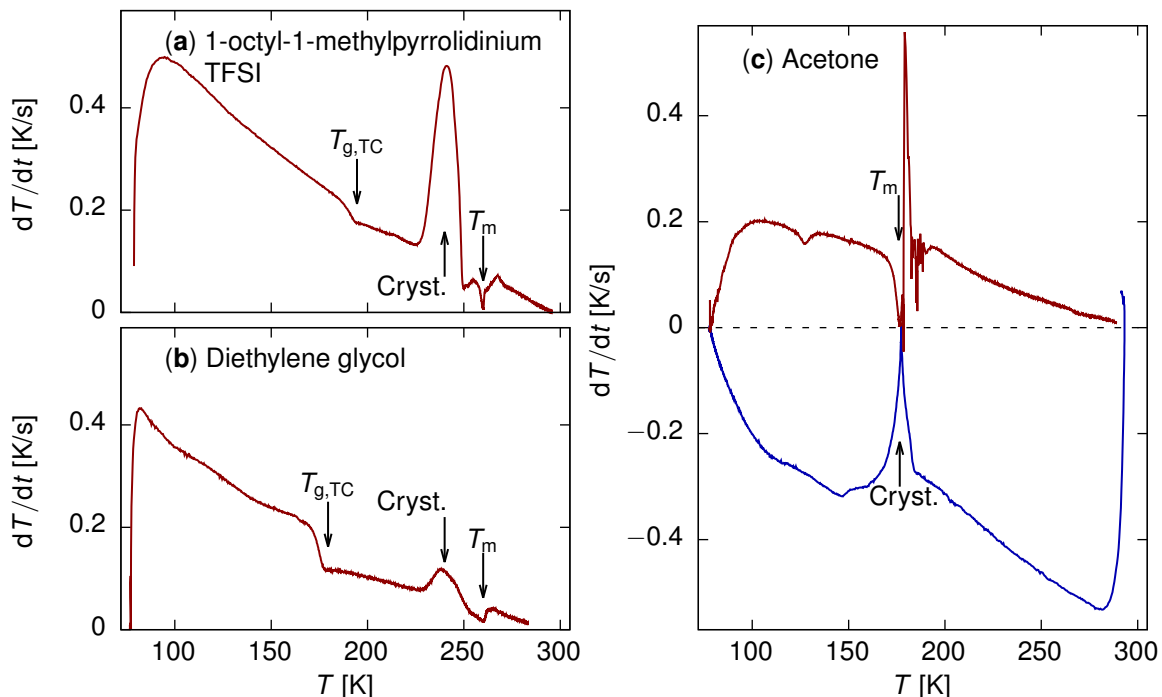


FIG. 4. Crystallization, melting, and glass transition studied on three samples<sup>17</sup> by the TC technique (melting and glass-transition temperatures are given in Table II). (a) and (b)  $(T, \frac{dT}{dt})$ -trace for slow heating after fast quench showing glass transition, crystallization from the supercooled liquid, and melting. (c)  $(T, \frac{dT}{dt})$ -trace for slow cooling and subsequent slow heating, showing crystallization in cooling and melting in heating. See Sec. III C for a discussion of further features.

process as seen in the large increase in  $\frac{dT}{dt}$ ). Finally, the melting of the crystal is observed at as an endothermic process ( $T_m = 260$  K), seen as the sharp dip in  $\frac{dT}{dt}$  down to 0.

In heating, an exothermic process leads to a rather wide peak in the  $(T, \frac{dT}{dt})$ -trace, as the process increases the heating rate ( $\frac{dT}{dt}$ ) over the baseline behavior until all excess heat is released, and simultaneously increases  $T$ . Conversely, endothermic process leads to a sharp peak, as  $T$  is constant and  $\frac{dT}{dt} = 0$  until enough heat has been provided to the sample.

Figure 4(b) shows a similar curve for diethylene glycol, which has a more pronounced glass transition, but a much smaller exothermic signal from the crystallization and a not so well-defined melting. Although this is the typical behavior for molecular liquids, the TC technique gives a good estimate of the melting point and a simple test of the stability of the supercooled liquid against crystallization.

As a final example of a crystallizing liquid data on acetone are presented in Fig. 4(c), showing  $(T, \frac{dT}{dt})$ -traces for a slow cooling and subsequent slow heating. For most molecular liquids, crystallization is suppressed during cooling, even at moderately slow cooling rates (the rate used here is  $\approx 0.5$  K/s), but for acetone this is not the case, since acetone unavoidably crystallizes around its freezing point at the cooling rates TC realizes. On cooling we thus observe an exothermic transition around 177 K (blue curve) that corresponds to the crystallization point of pure acetone. On slow heating of the crystal (red curve) we observe an endothermic peak around 177 K that confirms the melting of crystalline phase of acetone. At slightly higher temperatures a narrow exothermic peak emerges followed by a region of small peaks. The origin of this is unclear, but the observation resembles additional crystallization and melting events. A weak signal is observed on heating (even more weak on cooling) at 130 K, which appears like a glass transition, however, in the crystalline phase. Acetone is known to have low-temperature thermal transitions<sup>35</sup>, the origin of which has been debated during the last decades (see, e.g., Ref. 33 and 36). It has been proposed that



an order-disorder transition or more complex phase transitions exists<sup>33,35</sup>, but it has also been argued that variation in the strength of the electrostatic interactions between polar groups along the crystalline lattice cause these transitions<sup>37</sup>. Dielectric spectroscopy on the crystal shows that a dielectric process exists in the crystalline phase<sup>38</sup>, showing that some dynamical processes are still active in the crystal, which indicates a plastic crystalline behavior. Altogether, this demonstrates that TC also can be used for “quick and dirty” investigations of complex phenomena.

Stability against crystallization is a complicated problem, and the above sketched experiments are by no means meant to represent all different ways crystallization can occur. Due to the simplicity of the TC setup, different types of crystallization experiments can be performed *ad hoc*, e.g., by keeping the liquid at isothermal conditions above  $T_g$  and studying whether excess heat is generated by crystallization in a subsequent heating.

#### IV. SUMMARY

We have presented the general principle of thermalization calorimetry (TC), a simple technique for investigating supercooling, glass transition, and crystallization of liquids. The key idea is to monitor  $(T, \frac{dT}{dt})$ -curves for a system in which the thermal input power is proportional to the temperature difference to the sample surroundings. Changes in specific heat, glass transition, exothermic, and endothermic processes all have a clear signal in the  $(T, \frac{dT}{dt})$ -curves.

Uses of the TC technique for locating the glass-transition temperature, studying stability against crystallization, determining the melting point, and studying complex crystallization behavior have been illustrated. The TC technique should not be seen as a way to determine  $T_g$  and  $T_m$  precisely, which in any case is not possible for  $T_g$  (see table I and Ref. 21), but rather as a quick way of getting a good estimate of such quantities as well as, e.g., ratios of specific heat between solid and liquid.

An advantage of the TC technique is that it can easily be adopted to different experimental situations. By changing the temperature of the environment and the insulation used, different temperature regimes and different cooling-rate regimes can be explored. A straightforward modification of the TC technique is to use an oven as outer temperature, in this way allowing for studying substances with high  $T_g$  and  $T_m$  applicable, e.g., for many substances used in food science (as sugar and cocoa butter). By changing the thermometer type the TC technique can also be adopted to lower temperatures where thermocouples are less efficient.

TC can be realized in a variety of ways; all that is needed is a recording of  $T$  and  $\frac{dT}{dt}$ . Initially, we used analog electronics for the computations, with the later addition of a build-in ADC (Analog to Digital Converter) for recording the signal. With the development of good and cheap high resolution ADCs and small microcontrollers it is now possible to make a fully digital version with a high degree of flexibility, which can easily be built, e.g., for educational purposes. In summary, the TC technique is useful for initial studies of glass-forming liquids, as a test of new liquid, as well as for teaching purposes for instance in student projects.

#### ACKNOWLEDGMENTS

All students and staff at IMFUFA who have worked with and improved the TC-technique over the last 40 years, are gratefully acknowledged for helping in making the TC-technique a standard (workhorse) technique in our lab. This work was supported by the Danish National Research Foundation via grant DNRF61.

## Appendix A: Experimental details

This Appendix provides details on the experimental protocols used for TC measurements; sources of uncertainty are also discussed.

In all experiments the liquid is positioned in a small glass tube (8 mm in diameter and 40 mm in length). The thermocouple is fed through a hole in a soft silicon plug, which allows for a tight sealing when placed in the beaker (Fig. 5). The thermocouple junction should not touch the beaker and be positioned as close as possible to the middle of the beaker. Liquid nitrogen is used as cooling agent. The experiment normally takes place at room temperature. For slow heating a block of expanded polystyrene with approximately 5 cm wall thickness is used as insulating material (Fig. 5). With these dimensions initial heating rates of a few tenths of Kelvin per second ( $\approx 10\text{K}/\text{min}$ ) are typically obtained.

In the slow-cooling protocol the insulation consists of a slightly larger test tube simply lined with paper, by which cooling rates of order 0.5 K/s are obtained. As in the case of heating, the cooling rate may be varied by changing the insulation material.

The experimental protocol for slow heating after an initial quench is as follows:

1. The sample beaker with liquid is quench cooled directly in liquid nitrogen until it has been thermalized.
2. The block of expanded polystyrene is precooled by placing a beaker filled with liquid nitrogen in the block for time long enough to establish a stationary temperature gradient throughout the insulation block (with our dimensions, approximately 5 minutes).
3. The precooling beaker is removed, the sample beaker transferred from the liquid nitrogen Dewar to the block of expanded polystyrene, and a plug is inserted. This should be done as quickly as possible in order to minimize unintended heating of the sample and polystyrene block.
4.  $(T, \frac{dT}{dt})$  is recorded during the thermalization of the sample.

A number of sources of uncertainties can be identified:

- The specific heat is in general temperature dependent, limiting the temperature ranges over which a straight  $(T, \frac{dT}{dt})$ -trace can be expected.
- For slow heating experiments, a too short precooling time or too slow transfer of the sample to the block of expanded polystyrene lead to distortion of the first part of the heating curve, as Eq. (3) will not hold initially.
- The sample might be rather inhomogeneous after quench cooling (it normally fractures), leading to inhomogeneous conversion between the phases.
- Due to the size of the sample significant temperature gradients exist.
- For slow cooling it is often observed that the  $(T, \frac{dT}{dt})$ -trace does not point to  $(T_0, 0)$  in the low temperatures regime (as in Fig. 2(b)). This is attributed to inhomogeneous insulation of the sample.
- The heat capacity of the sample beaker will influence the measured specific heat.

## Appendix B: Details of our implementation of the TC technique

The TC technique can be implemented in different ways since the idea is simply to monitor  $T(t)$  with some type of thermometer and record  $(T, \frac{dT}{dt})$ . Two versions of the technique have been developed over the years at Roskilde University: An analog based and a digital based version. In the following the two methods are described briefly<sup>39</sup> and compared (see Fig. 6 for a schematic representation of the two implementations).

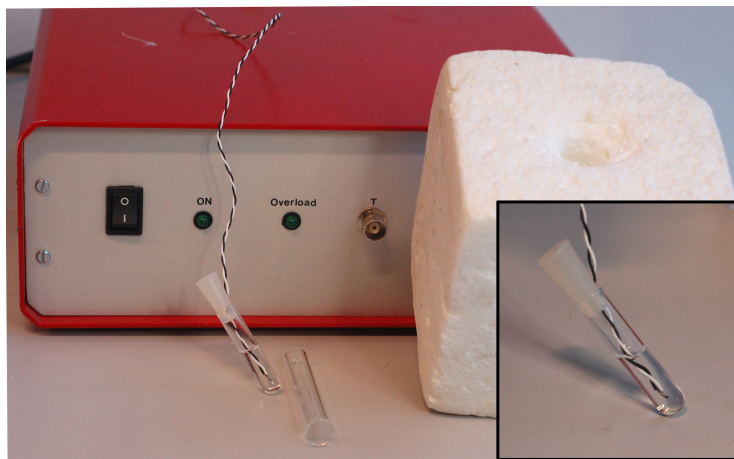


FIG. 5. Photo of the TC setup. Shown are the sample with thermometer (the thermocouple) (the inset), the insulation block of expanded polystyrene used for slow heating, the test tube, which filled with liquid nitrogen is inserted into the insulation block before the heating experiment for precooling the insulation block to establish the temperature gradient. Also, the analog TC box (known as the “Red box”) is seen. The analog TC box (Appendix B) normally communicates the digitized  $(T, \frac{dT}{dt})$  measurements to an attached PC over USB. However, an analog representation of the  $(T, \frac{dT}{dt})$  signal is also available.

Common to both version is that a “J” type thermocouple is used as thermometer. It has a reasonable sensitivity in the temperature range from room temperature ( $50 \mu\text{V/K}$ ) to liquid nitrogen temperature ( $20 \mu\text{V/K}$ ). A thermocouple has the advantage that the heat capacity of the thermometer itself is very small and that it is mechanically robust and cheap. Both implementations use a microcontroller for delivering the results to a PC in which the data are analyzed and visualized using the Matlab software package.

The analog implementation developed at Roskilde University approximately 40 years ago is based on analog electronics (Fig. 6(a)). It utilizes high-quality operation amplifiers (op-amp) for analog amplification, differentiation, and low-pass filtering of the thermocouple signal, and it has analog reference-point temperature compensation. Originally the analog output signal proportional to  $(v, \frac{dv}{dt})$  (where  $v$  is the thermovoltage) was visualized by means of an “XY-plotter”. Currently, the analog signal is digitized using a high resolution analog-to-digital converter (ADC) connected to a microcontroller that communicates the result to a PC. In the control and visualization software the thermovoltage  $(v(t))$  and its time derivative  $(\frac{dv}{dt})$  are converted to actual temperature  $(T)$  and temperature rate  $(\frac{dT}{dt})$ . The data presented in this paper are obtained using this version of the TC technique.

The analog version has good resolution and low noise. However, it requires the ability to build custom-made electronic circuits, which might be out of range for some applications, e.g. for use in high-school physics education. The digital version takes advantage of the fact that inexpensive, high-quality microcontrollers and ADC’s have become available in recent years.

Our digital TC-technique implementation uses the LTC2983 “Multi-Sensor High Accuracy Digital Temperature Measurement System” chip (Linear Technology). The LTC2983 has the advantage that thermocouples (and other commonly used types of thermometers) can be directly connected to the chip; the signal is measured by a high-quality 24-bit ADC. Furthermore, the LTC2983 has multiple input channels, allowing for easy digital “reference junction compensation” by having a second thermometer measuring the temperature of the “reference junction”.

The LTC2983 is available on a demo board for which “daughter boards” for different thermometers (including thermocouples) are available, which easily connect to a microcontroller<sup>41</sup>. These three boards (LCT2983 demo board, thermocouple daughter

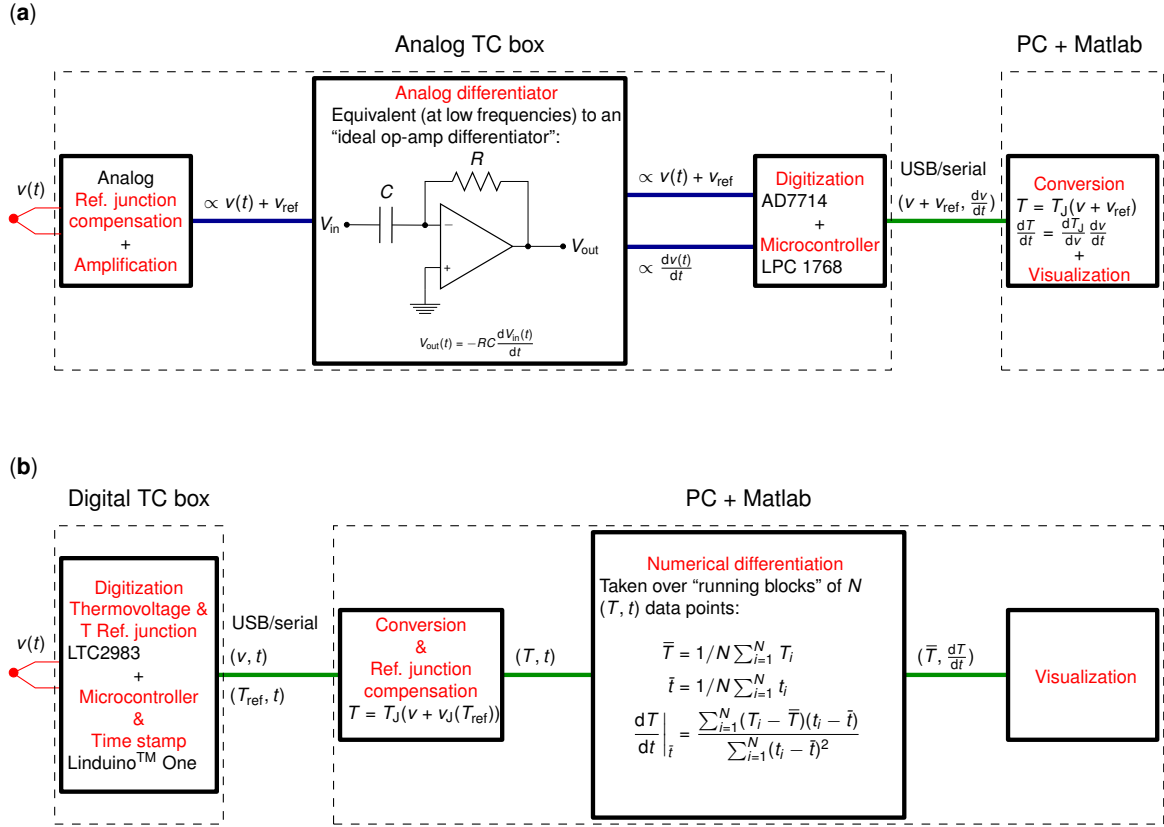


FIG. 6. Schematic representation of two version of the TC-technique.  $v$  is the thermovoltage,  $v_{\text{ref}}$  the thermovoltage associated with the reference junction temperature relative to  $0^\circ\text{C}$ ,  $T_J(v)$  the conversion function<sup>40</sup> between (reference point compensated) thermovoltage and temperature (and  $v_J(T)$  the inverse function). Analog quantities are designated as time dependent, e.g.,  $v(t)$ , digitized quantities as pairs, e.g.,  $(v, t)$ . **(a)** The original analog-based TC-technique implementation consisting of an “Analog TC-box” (Fig. 5) which performs analog signal processing and differentiation of the thermovoltage. The analog signals are digitized by a high-quality ADC and the results communicated to a PC by a microcontroller, where it converted into temperature for visualization and analysis. **(b)** Digital TC-technique implementation consisting of a “Digital TC-box” (see Appendix B for details), which digitizes the thermovoltage and reference point temperature and communicates the measurements together with time stamps via a microcontroller to the PC. Averaging, differentiation, and visualization is done on the PC.

board, and microcontroller) provides a full TC system.

The LTC2983 is configured to give the raw digitized thermovoltage without performing any automated reference junction compensation (this introduces additional noise in the temperature signal) or using the internal table for converting thermovoltages to temperature (this was found not to work well at low temperatures). Including time for communicating results to the PC, the measuring frequency is  $\approx 5.8\text{Hz}$ . The temperature of the “reference junction” is measured every  $\approx 7\text{s}$ ; for the presented data the “reference junction” temperature was to a good approximation temperature independent. Besides controlling the LTC2983 and communicating with the PC the microcontroller also time stamps all measurements.

The  $(T, \frac{dT}{dt})$  data are found by calculating mean and linear-regression slope over “running blocks” of  $N$   $(t, T(t))$  data points. To obtain data of comparable quality to those of the analog version of TC-technique, the averaging and slope calculations is done over blocks of  $N = 60$  points corresponding to averaging over  $\approx 10\text{s}$ . With this block size the standard derivation of the slope becomes of order  $(1-2) \times 10^{-3}\text{K/s}$ . Larger  $N$  smears our the  $(T, \frac{dT}{dt})$ -

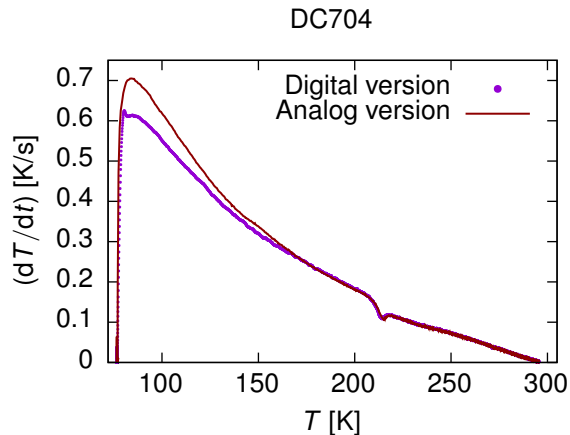


FIG. 7. Comparison of the analog and digital versions of the TC technique applied to a slow heating of an initially quenched sample of the glass-forming liquid DC704.

trace, smaller  $N$  introduces more noise.

Figure 7 shows a comparison of the data obtained by the analog and digital versions of the TC technique, demonstrating consistent results.

If a shorter averaging time is desired, e.g., for monitoring relatively fast processes, a simple amplifier can easily be added to the the digital TC implementation. Using a high-quality op-amp in a standard inverting amplifier configuration<sup>42</sup>, the necessary averaging is reduced to  $N = 20$  points (corresponding to  $\approx 3.3$ s) for noise levels in the slope of order  $(1-2) \times 10^{-3}$  K/s.

### Appendix C: A simple model for understanding the TC signal of a glass-forming liquid

In this section we briefly discuss a simple model that can be used for interpreting the results from the TC technique when applied to glass-forming liquids. The model is based on the old understanding of Tool and others<sup>13</sup> that structure may be quantified in terms of a so-called fictive temperature<sup>16</sup>. This is the temperature at which the liquid’s structure is identical to that of the glass; thus for the metastable supercooled liquid the fictive temperature,  $T_f$ , is the actual temperature, whereas below the glass transition  $T_f$  is constant, equal to the glass transition temperature. For annealing just below the glass transition the structure gradually changes and the fictive temperature moves slowly towards the annealing temperature.

In the network representation of the model voltages correspond to temperatures and electrical currents to heat currents. Specific heat is represented as capacitors and thermal resistance as resistors. Figure 8(a) shows an electrical network analog of the model and Fig. 8(b) shows typical heating and cooling curves obtained by solving the model.

The specific heat can be separated into two parts: an “instantaneous” contribution,  $C_i$ , which is able to take up heat without structural rearrangement of the molecules; this corresponds to the high-frequency limit of the dynamic specific heat, and a structural contribution,  $C_s$ .

The major characteristic of a glass-forming liquid is that the time scale separating the instantaneous and structural contributions to relaxation phenomena increases dramatically when decreasing the temperature<sup>16</sup>. This is reflected in the model by the temperature-dependent resistor  $R_s(T)$ , which in this simple model is taken to be Arrhenius (generally, molecular glass-forming liquids have non-Arrhenius behavior<sup>16,44</sup>):

$$R_s(T) = R_\infty e^{T_a/T}. \quad (\text{C1})$$

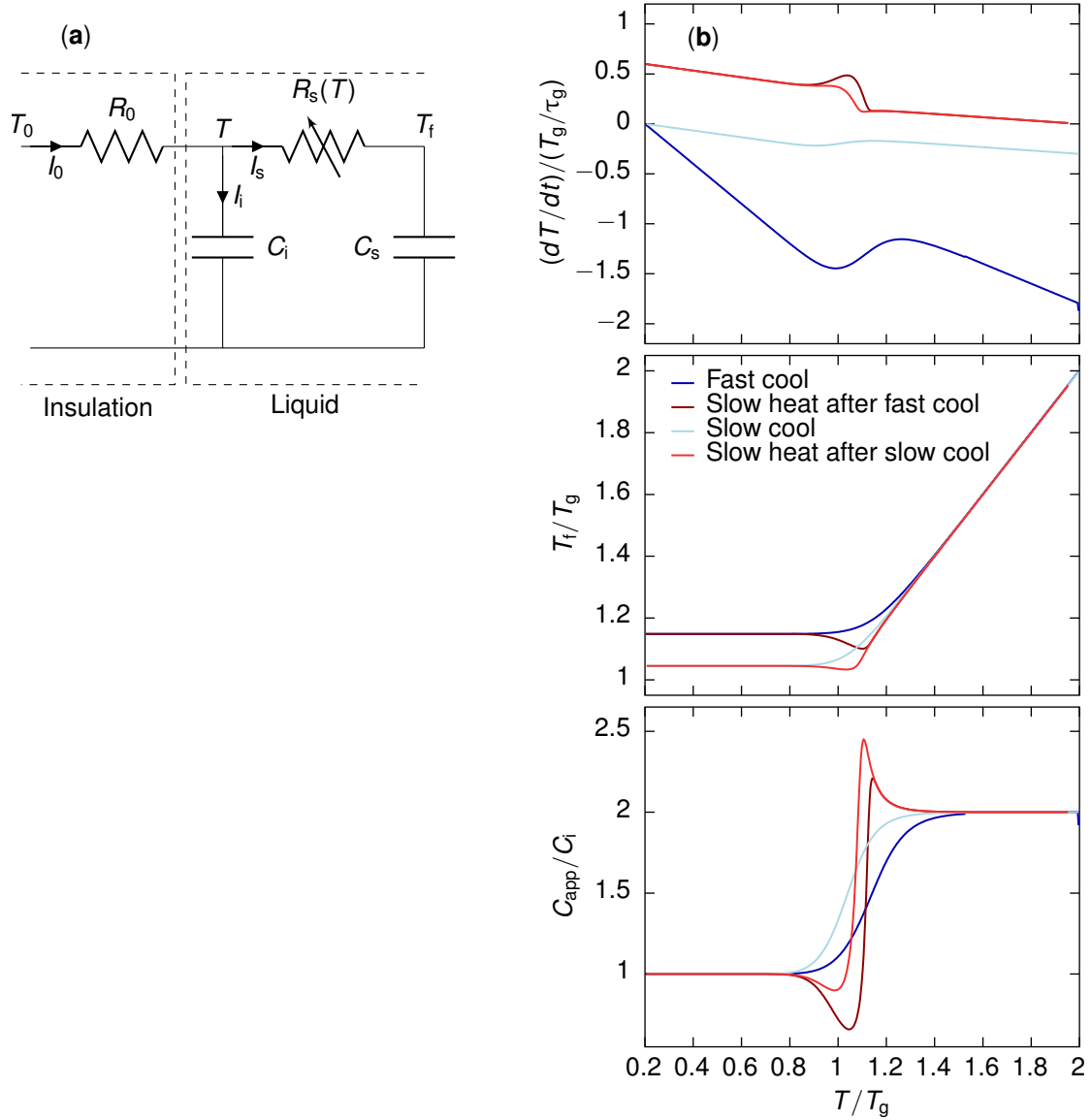


FIG. 8. The simple model for understanding the TC signal from a glass-forming liquid described in Appendix C (Eqs. (C1) and (C2)). **(a)** Electrical network representation of the model. Voltages represent temperatures, electrical currents represent thermal currents, resistors represent thermal resistance, and capacitors represent specific heat. **(b)** Results from model calculations by simple Euler integration using the implementation shown in Fig. 9 and the parameters given in Ref. 43.  $C_{app}$  is the apparent specific heat as it would be observed by the TC technique.

From the network it is seen that when the fictive temperature ( $T_f$ ) is identical to the actual temperature of the system ( $T$ ) the system is in equilibrium and there is no current in the  $R_s$  resistor, corresponding to no exchange of energy between the instantaneous and the structural degrees of freedom.

In order to model the results of TC experiments the model also includes the outer environment temperature,  $T_0$ , and the thermal resistance to the surroundings,  $R_0$ , (according to Eq. (3)).

The model can be expressed as a system of two non-linear Tool-type coupled differential

```

function [T_array , Tf_array , dTdt_array , t_array , C_app_array]=...
    TC_Model_Euler(T_init , Tf_init , tau_0 , C , Ta , T0 , dt , t_end)
% All variable are in dimensionless units

%calculate time array
t_array=0:dt:t_end;

% initialize output arrays
T_array=zeros(size(t_array));
Tf_array=zeros(size(t_array));
dTdt_array=zeros(size(t_array));
C_app_array=zeros(size(t_array));

% use initial conditions
T=T_init;
Tf=Tf_init;

% Euler integration of the model
for k=1:length(t_array)
    % calculate tau_s including
    % a high temperature cut off
    tau_s=max(tau_0*1e-3,exp(Ta.*(1./T-1)));

    % calculate the time derivatives
    dTdt=(T0-T)./tau_0-(T-Tf).*C./tau_s; % dT/dt
    dTfdt=(T-Tf)./tau_s; % dTf/dt

    % update temperatures
    T=T+dTdt*dt;
    Tf=Tf+dTfdt*dt;

    % update apparent specific heat
    % (normalized to C_i)
    C_app=-(T-T0)./dTdt/tau_0;

    % store results for output
    T_array(k)=T;
    Tf_array(k)=Tf;
    dTdt_array(k)=dTdt;
    C_app_array(k)=C_app;
end

```

FIG. 9. Matlab/octave code for numerical integration of the model given by Eq. (C4) and illustrated in Fig. 8(a).

equations involving the sample temperature,  $T$ , and the fictive temperature,  $T_f$ :

$$\frac{dT(t)}{dt} = \frac{I_0 - I_s}{C_i} = \frac{T_0 - T}{R_0 C_i} - \frac{T - T_f}{R_s(T) C_i} \quad (\text{C2a})$$

$$= \frac{T_0 - T}{\tau_0} - \frac{T - T_f}{\tau_s(T)} \tilde{C} \quad (\text{C2b})$$

$$\frac{dT_f(t)}{dt} = \frac{I_s}{C_s} = \frac{T - T_f}{R_s(T) C_s} = \frac{T - T_f}{\tau_s(T)}, \quad (\text{C2c})$$

where  $\tau_0 = R_0 C_i$  is the characteristic time of the TC-technique,  $\tau_s(T) = R_s(T) C_s$  the characteristic relaxation time of the specific heat (separating instantaneous and structural degrees of freedom), and  $\tilde{C} = C_s / C_i$  the ratio between structural and instantaneous components to the specific heat.

The structural characteristic time can be rewritten as:

$$\tau_s(T) = C_s R_s(T) = C_s R_\infty e^{T_a/T} = \tau_g e^{T_a(1/T - 1/T_g)} \quad (\text{C3})$$

where  $T_g$  is the glass-transition temperature and  $\tau_g$  is the corresponding relaxation time.

By choosing  $\tau_g$  and  $T_g$  as units for time and temperature, respectively, the above set of equations can be brought to dimensionless form:

$$\frac{d\tilde{T}}{d\tilde{t}} = \frac{\tilde{T}_0 - \tilde{T}}{\tilde{\tau}_0} - \frac{\tilde{T} - \tilde{T}_f}{\tilde{\tau}_s(\tilde{T})} \tilde{C} \quad (\text{C4a})$$

$$\frac{d\tilde{T}_f}{d\tilde{t}} = \frac{\tilde{T} - \tilde{T}_f}{\tilde{\tau}_s(\tilde{T})} \quad (\text{C4b})$$

$$\tilde{\tau}_s(\tilde{T}) = e^{\tilde{T}_a(1/\tilde{T}-1)} \quad (\text{C4c})$$

The model described by Eq. (C4) can be numerically integrated by simple Euler integration. The Matlab function shown in Fig. 9 performs the integration and Fig. 8(b) shows results from such model calculations.

This model is the simplest possible model for the specific heat of a glass-forming liquid (it predicts a Debye-type equilibrium frequency-dependent specific heat at variance with experiments (e.g. Refs. 45 and 46)). The model nevertheless captures qualitatively the shapes of the  $(T, \frac{dT}{dt})$ -traces, both on cooling and heating, As well as the difference between slow heating after slow and fast cooling, compare Figs. 8(b) and 2(b).

- <sup>1</sup>G. T. Armstrong, *J. Chem. Educ.* **41**, 297 (1964).
- <sup>2</sup>P. L. Privalov and S. A. Potekhin, “[2] Scanning microcalorimetry in studying temperature-induced changes in proteins,” in *Enzyme Structure Part L*, Methods in Enzymology, Vol. 131, edited by C. H. W. Hirs and S. N. Timasheff (Academic Press, 1986) pp. 4 – 51.
- <sup>3</sup>E. Gmelin, *Thermochim. Acta* **304/305**, 1 (1997).
- <sup>4</sup>C. Schick, D. Lexa, and L. Leibowitz, “Differential scanning calorimetry and differential thermal analysis,” in *Characterization of Materials* (2002) pp. 1–13.
- <sup>5</sup>B. Wunderlich, *Thermal Analysis of Polymeric Materials* (Springer, 2005).
- <sup>6</sup>M. Reading and D. J. Hourston, eds., *Modulated Temperature Differential Scanning Calorimetry*, Hot Topics in Thermal Analysis and Calorimetry, Vol. 6 (Springer, 2006).
- <sup>7</sup>E. Zhuravlev and C. Schick, *Thermochim. Acta* **505**, 1 (2010).
- <sup>8</sup>B. Zhao, L. Li, F. Lu, Q. Zhai, B. Yang, C. Schick, and Y. Gao, *Thermochim. Acta* **603**, 2 (2015).
- <sup>9</sup>C. Schick and G. Höhne, eds., *Thermochimica Acta: Special issue on Chip Calorimetry*, Vol. 603 (Elsevier B.V., 2015).
- <sup>10</sup>V. Mathot, M. Pyda, T. Pijpers, G. V. Poel, E. van de Kerkhof, S. van Herwaarden, F. van Herwaarden, and A. Leenaers, *Thermochim. Acta* **522**, 36 (2011).
- <sup>11</sup>Center for Viscous Liquid Dynamics: “Glass and Time”. <http://glass.ruc.dk>.
- <sup>12</sup>J. H. Jensen, *Fysisk Tidsskrift* **70**, 174 (1972), (In Danish).
- <sup>13</sup>A. Q. Tool, *J. Am. Ceram. Soc.* **29**, 240 (1946).
- <sup>14</sup>For initial temperature of the sample  $T_{\text{initial}}$  the solution of Eq. (4) is  $T(t) = T_0 + e^{-\frac{t}{R_0 C}} (T_{\text{initial}} - T_0)$ .
- <sup>15</sup>W. Kauzmann, *Chem. Rev.* **43**, 219 (1948).
- <sup>16</sup>J. C. Dyre, *Rev. Mod. Phys.* **78**, 953 (2006).
- <sup>17</sup>DC704 is the Dow Corning® diffusion pump oil: tetramethyl-tetraphenyl-trisiloxane. Glycerol (propane-1,2,3-triol) is a standard Flukar® glycerol. 1-octyl-1-methylpyrrolidinium TFSI is the ionic liquid 1-octyl-1-methylpyrrolidinium bis(trifluoromethanesulfonyl)imide acquired from Solvionic. Diethylene glycol is standard quality. Acetone is of standard laboratory solvent quality.
- <sup>18</sup>T. Christensen and N. B. Olsen, *J. Non-Cryst. Solids* **172–174**, 357 (1994).
- <sup>19</sup>B. Jakobsen, K. Niss, and N. B. Olsen, *J. Chem. Phys.* **123**, 234511 (2005).
- <sup>20</sup>D. Gundermann, U. R. Pedersen, T. Hecksher, N. P. Bailey, B. Jakobsen, T. Christensen, N. B. Olsen, T. B. Schröder, D. Fragiadakis, R. Casalini, C. M. Roland, J. C. Dyre, and K. Niss, *Nat. Phys.* **7**, 816 (2011).
- <sup>21</sup>B. Jakobsen, T. Hecksher, T. Christensen, N. B. Olsen, J. C. Dyre, and K. Niss, *J. Chem. Phys.* **136**, 081102 (2012).
- <sup>22</sup>T. Hecksher, N. B. Olsen, K. A. Nelson, J. C. Dyre, and T. Christensen, *J. Chem. Phys.* **138**, 12A543 (2013).
- <sup>23</sup>A. Sanz, (2015), Unpublished data.
- <sup>24</sup>T. E. Christensen, *Tekster fra IMFUFA* **184** (1984), (In Danish); N. O. Birge and S. R. Nagel, *Phys. Rev. Lett.* **54**, 2674 (1985); O. Yamamuro, Y. Oishi, M. Nishizawa, and T. Matsuo, *J. Non-Cryst. Solids* **235–237**, 517 (1998); E. Donth, *The Glass Transition — Relaxation Dynamics in Liquids and Disordered Materials*, Springer Series in Materials science No. 48 (Springer, Berlin, 2001); O. Andersson and G. P. Johari, *J. Chem. Phys.* **144** (2016).
- <sup>25</sup>The timescales are defined as  $\tau = 1/(2\pi\nu_p)$ , where  $\nu_p$  is the frequency at maximum loss in isothermal measurements of the frequency dependent complex response functions. Data on the characteristic



- timescale as function of temperature have been extrapolated down to  $\tau = 100$  s by linear extrapolation of  $(T, \log \tau)$  data.
- <sup>26</sup>T. Sato and R. Buchner, *J. Chem. Phys.* **118**, 4606 (2003).
- <sup>27</sup>K. Murata and H. Tanaka, *Nat. Mater.* **11**, 436 (2012).
- <sup>28</sup>K. Amann-Winkel, R. Böhmer, F. Fujara, C. Gainaru, B. Geil, and T. Loerting, *Rev. Mod. Phys.* **88**, 011002 (2016).
- <sup>29</sup>R. W. Salt, *Annu. Rev. Entomol.* **6**, 55 (1961).
- <sup>30</sup>P. Davis-Searles, A. Saunders, D. Erie, D. Winzor, and G. Pielak, *Annu. Rev. Biophys. Biomol. Struct.* **30**, 271 (2001).
- <sup>31</sup>P. G. Debenedetti, *J. Phys.: Condens. Matter* **15**, R1669 (2003).
- <sup>32</sup>W. M. Haynes, ed., *CRC Handbook of Chemistry and Physics*, 96th ed. (CRC Press, 2015).
- <sup>33</sup>R. M. Ibberson, W. I. F. David, O. Yamamuro, Y. Miyoshi, T. Matsuo, and H. Suga, *J. Phys. Chem.* **99**, 14167 (1995).
- <sup>34</sup>K. Adrjanowicz, K. Kaminski, M. Paluch, and K. Niss, *Cryst. Growth Des.* **15**, 3257 (2015).
- <sup>35</sup>K. K. Kelley, *J. Am. Chem. Soc.* **51**, 1145 (1929).
- <sup>36</sup>S. Shin, H. Kang, J. S. Kim, and H. Kang, *J. Phys. Chem. B* **118**, 13349 (2014).
- <sup>37</sup>D. R. Allan, S. J. Clark, R. M. Ibberson, S. Parsons, C. R. Pulham, and L. Sawyer, *Chem. Commun.*, 751 (1999).
- <sup>38</sup>A. Sanz, D. Rueda, A. Nogales, M. Jiménez-Ruiz, and T. Ezquerra, *Physica B* **370**, 22 (2005).
- <sup>39</sup>Details, schematics and software associated with the TC-implementations are available on request.
- <sup>40</sup>M. C. Croarkin *et al.*, “Temperature-electromotive force reference functions and tables for the letter-designated thermocouple types based on the ITS-90,” (NIST, 1993) Chap. Revised Thermocouple Reference Tables: Type J.
- <sup>41</sup>The boards used from Linear Technology for the digital TC-implementation are: DC2209 (main demo circuit containing the LTC2983), DC2212 (Thermocouple Daughter Board), and DC2026 (Linduo™ One, Arduino compatible microcontroller).
- <sup>42</sup>The amplifier utilized for the digital TC implementation is based on the Analog Devices AD8571 op-amp. This is a single supply (5 V), ultra low noise, zero drift op-amp. The op-amp was powered from the 5 V supply on LTC2983 demo board. A standard inverting amplifier configuration was used with a passive low-pass filter on the input and 255.5 times amplification.
- <sup>43</sup>Model parameters used for the integration of Eq. C4 to give the results presented in Fig. 8(b) are:  $\tilde{T}_{\text{room}} = 2$ ,  $\tilde{T}_{\text{cool}} = 0.2$ ,  $\tilde{C} = 1$ ,  $\tilde{T}_a = 20$ ,  $\tilde{\tau}_{0,\text{fast}} = 0.5$ ,  $\tilde{\tau}_{0,\text{slow}} = 3$ . For cooling, the system is assumed to be initial in equilibrium ( $\tilde{T} = \tilde{T}_f = \tilde{T}_{\text{room}}$ ). The final values from the cooling is used as initial condition for the heating. The integration was performed using the function presented in Fig. 9 using a time step size of 0.0001.
- <sup>44</sup>T. Hecksher, A. I. Nielsen, N. B. Olsen, and J. C. Dyre, *Nat. Phys.* **4**, 737 (2008).
- <sup>45</sup>T. Christensen, *J. Phys. (Paris), Colloq.* **46**, C8:635 (1985).
- <sup>46</sup>N. O. Birge, P. K. Dixon, and N. Menon, *Thermochim. Acta* **304–305**, 51 (1997).